Mechanosensitive Osteogenesis on Native Cellulose Scaffolds for Bone Tissue Engineering.

Maxime Leblanc Latour[1] and Andrew E. Pelling[1,2,3]

[1] Department of Physics, STEM Complex, 150 Louis Pasteur, University of Ottawa, Ottawa, ON, K1N 6N5, Canada
[2] Department of Biology, Gendron Hall, 30 Marie Curie, University of Ottawa, Ottawa, ON, K1N 6N5, Canada
[3]Institute for Science, Society and Policy, Desmarais Building, 55 Laurier Ave. East, University of Ottawa, Ottawa, ON, K1N 6N5, Canada

Author for correspondence: a@pellinglab.net.

Abstract

Accurate physical representation of the tissue microenvironment is essential for implant development. In this study, we applied cyclic hydrostatic pressure (HP) to mimic the effect of cyclic hydrostatic pressure (HP) in a bone-like environment, using a custom-made, remote controlled bioreactor. In recent years, plant-derived cellulosic biomaterials have become a popular way to create scaffolds for a variety of tissue engineering applications. Moreover, such scaffolds possess similar physical properties (porosity, stiffness) that resemble bone tissues and have been explored as potential biomaterials for tissue engineering applications. Here, plant-derived cellulose scaffolds (derived from apple hypanthium tissue) were seeded with MC3T3-E1 pre-osteoblast cells. After 1 week of proliferation, cell-seeded scaffolds were exposed to HP up to 270 KPa at a frequency of 1Hz, once per day, for up to 2 weeks. Scaffolds were incubated in osteogenic inducing media or regular culture media. The effect of cyclic hydrostatic pressure combined with osteogenic inducing media on cell-seeded scaffolds resulted in an increase of differentiated cells. This corresponded with an upregulation of alkaline phosphatase activity and scaffold mineralization. The results reveal that in vitro, the mechanosensitive pathways which regulate osteogenesis appear to be functional on novel plant-derived cellulosic biomaterials.

Introduction

Upon injury or break, bone have the ability of self renewal. However, large defect created by either injury or disease may require graft placement to avoid non-union or malunion of the bone tissue (Andrzejowski and Giannoudis, 2019). Such grafts can be derived from the patient's own body (autologous grafts), usually the iliac crest, and it's considered the "gold standard" in regenerative orthopedics (Campana et al., 2014; Parikh, 2002; Sakkas et al., 2017; Wang and Yeung, 2017). However, limited size grafts, donor site morbidity and infections, cost and post-operative pain at both donor and receiver site may lead to alternative for the graft (Parikh, 2002; Wang and Yeung, 2017): from a cadaver donor (allograft), from animal sources (xenograft), or artificially derived (alloplastic). Such alternatives all have their own benefits and drawback, the later however provides a potential alternative with lower risk of transmitted diseases and infections , as well as

overcoming the size limitation barrier (Parikh, 2002; Wang and Yeung, 2017) . Alloplastic graft is also considered a more ethical alternative than allografts and xenografts (Fernández et al., 2015). Physical properties are key parameters for alloplastic grafts development, such as pore size, pore interconnectivity and elastic modulus (Campana et al., 2014; Gao et al., 2019; Nukavarapu et al., 2015). Fine tuning of these parameters leads to better mechanical support, stability of the implant and lead to improved osteoconductivity and osteoinductivity. Thus, designing such material for bone tissue engineering (BTE) applications requires fine tuning according to the surrounding environment.

Long bones are highly dynamic structural tissues, with functions ranging from body support to physical locomotion. A whole spectrum of forces is acting on different area of the skeletal system. For instance, the pressure found in femur head in human adult can reach 5 MPa during normal locomotion, and can reach up to 18 MPa for other activities (Morrell et al., 2005). On a microscopic level, these forces are transmitted to the osteocytes through Wnt/β-catenin mechano-sensing pathways in the lacuna-canaliculi network (Bonewald and Johnson, 2008). Such force-regulated mechanisms lead to formation and removal of bone tissue, trough bone remodeling processes (Bonewald and Johnson, 2008). It's been shown that the pressure inside the lacuna-canaliculi network is around 280 kPa (Zhang et al., 1998). In recent years, multiple bioreactors were developed to apply stresses to cultured osteoblast cells (and their underlying substrate) to better replicate native bone environment. Such bioreactors can apply contact uniaxial compression/tension , contact biaxial compression/tension , flow inducing shear-stress , mechanical shear stress electrical or a combination of these stimuli (Brunelli et al., 2019; Pörtner et al., 2005). Also, bioreactors applying static or cyclic hydrostatic pressure by compressing the gas phase above incompressible media, or by direct compression of the medium were used on seeded cells (Gardinier et al., 2009; Henstock et al., 2013; Liu et al., 2010; Reinwald et al., 2015; Reinwald and El Haj, 2018; Stavenschi et al., 2018; Zhao et al., 2015). In addition to mechanical stimulus, three-dimensional culturing of the cells is critical for better representing the in vivo conditions. With a specific tissue-oriented scaffold structure (or biomaterial) and appropriate applied mechanical stimuli one can expect better osteointegration and overall performance *in vivo*.

A wide variety of three-dimensional biomaterials have been utilized support the growth and proliferation of cells in environments that mimic bone tissues. Commonly used biomaterials for BTE include inorganic calcium-based materials such as hydroxyapatite (HA), tricalcium phosphate, bioceramics or bioactive glass (Wang and Yeung, 2017). These types of materials are osteoconductive, can promote osteointegration and provide structural support at the implant site (Wang and Yeung, 2017). However, they show poor osteoconduction and little osteogenesis response (Wang and Yeung, 2017). Alternatively, Polymer-derived biomaterials such as poly(glycolic acid) (PGA), poly(lactic acid) (PLA) and poly(ε-caprolactone) (PCL) are alternatively used (Wei et al., 2020). PGA, PLA and PCL have proven to be biocompatible, with suitable mechanical properties for BTE (Wei et al., 2020). Moreover, polymer based scaffolds have a tunable degradation rate and can be chemically modify to change the surface chemistry (Wei et al., 2020). However, the degradation of the implanted scaffolds creates acidic bi-products which can lead to an inflammatory response and decrease the efficiency bone repair (Wei et al., 2020). Finally, naturally occurring polymers such as collagen, chitosan and silk are also use for BTE research and clinical applications (Wei et al., 2020). Collagen account for 90% the organic constituents in bone matrix (Lee and Volpicelli, 2017). However, due to its poor mechanical properties and structural stability, collagen cannot be used as a standalone scaffold and often needs to be combine with another material (e.g. HA, bioceramics) (Lee and Volpicelli, 2017; Wei et al., 2020). Chitosan-derived scaffolds have also shown to promote osteoblast differentiation and mineralization and can be combined with other material to enhance mechanical properties

and efficiency (Di Martino et al., 2005; Wei et al., 2020). Silk degradation by-products are biocompatible, has better mechanical properties than Collagen and Chitosan for BTE applications and can promotes osteogenic factors (Wei et al., 2020). Finally, cellulose is also naturally derived polymer that has been shown to be effective in BTE applications (Hickey and Pelling, 2019; Lee et al., 2019; Torgbo and Sukyai, 2018). Cellulose is a long chain polysaccharide consisting of repeating glucose sub-units connected via β(1 -> 4) glycosidic bonds. Cellulose is synthetized by plants as a structural component of their cell wall and is also synthesised by certain types of bacteria.

Previous studies by our group and others, have shown that porous, cellulose or chitin based scaffolds derived from plants or fugus can be used as tissue engineering scaffolds (Gershlak et al., 2017; Hickey et al., 2018; Lee et al., 2019; Modulevsky et al., 2016, 2014). Moreover, these biomaterials can be sourced from plants that closely matches the microstructure of the tissue to be replicated (Hickey et al., 2018). Successful experiments *in vitro* and *in vivo* showed that these biomaterials can host various cell types , are biocompatible and supports active angiogenesis (Hickey et al., 2018; Modulevsky et al., 2016, 2014). Plant-derived biomaterials can also be functionalised with peptides or biomineralized for better cell attachment (Fontana et al., 2017). Due to their pore size and pore interconnectivity, cellulose-based scaffolds derived from apples have been used for cell differentiation into osteoblasts (Lee et al., 2019). Building upon these initial discoveries, other groups have successfully differentiated human pluripotent stem cells into bone-like tissues within scaffolds derived from decellularized mushroom or apple tissues (Lee et al., 2019). More importantly, the clinical potential of these scaffolds has been examined by implanting disk-shaped scaffolds in cranial defects in rats (Lee et al., 2019). Their findings showed partial bone regeneration within the implant after 8 weeks, type 1 collagen deposition and blood vessel formation (Lee et al., 2019). However, to date, the mechanobiology of cells cultured on plant-derived scaffolds has not been examined in any detail. It remains is poorly understood how these critical signal transduction pathways are, or are not, impacted when cultured on unconventional plant-derived cellulosic biomaterials. Here, to examine the potential role plant-based biomaterials can play in BTE applications, we explore how mechanical stimulation impacts the differentiation of pre-osteoblasts when cultured on plant cellulose scaffolds. In a custom-built bioreactor, we apply cyclic hydrostatic pressure stimulation to differentiating osteoblasts and examine the regulation of key markers of osteogenesis and mineralization. The results reveal that application of hydrostatic pressure, in combination with osteogenic inducing media, leads to enhanced differentiation. This work provides further evidence that plant-derived cellulose scaffolds support osteogenesis and have potential applications in BTE in the long term.

Materials and Methods

Scaffold fabrication

Samples were prepared following established protocols (Hickey et al., 2018; Modulevsky et al., 2016, 2014). Briefly, MacIntosh apples (Canada Fancy) were cut with a mandolin slicer to 1 mm-thick slices. A biopsy punch was used to create 5 mm-diameter disks in the hypanthium tissue of the apple slices. The disks were decellularized in a 0.1% sodium dodecyl sulfate solution (SDS, Fisher Scientific, Fair Lawn, NJ) for two days. Then, the decellularized disks were gently washed in deionized water, before incubation in 100 mM $CaCl_2$ for two days. The samples were sterilized with 70% ethanol for 30 min, gently washed in deionized water, and placed in a 96-well culture plate prior to cell seeding.

MC3T3-E1 Subclone 4 cells (ATCC® CRL-2593™, Manassas, VA) (Quarles et al., 1992) were cultured and maintained in a humidified atmosphere of 95% air and 5% CO_2, at 37°C. The cells were cultured in Minimum Essential Medium (α-MEM, ThermoFisher, Waltham, MA), supplemented with 10% Fetal Bovine Serum (FBS, Hyclone Laboratories Inc., Logan, UT) and 1% Penicillin/Streptomycin (Hyclone Laboratories Inc). Cells were tryspinized and suspended in culture media. Scaffolds were placed individually in 96-well plates. Prior to cell seeding, scaffolds were immersed in culture media and incubated in a humidified atmosphere of 95% air and 5% CO_2, at 37°C, for 30 min. The culture media was completely aspirated from the wells. Cells were tryspinized and suspended and a 30 µL drop of cell culture suspension, containing $5 \bullet 10^4$ cells, was pipetted on each scaffold. The cells were left to adhere on the scaffolds for 2 hours before adding 200 µL of culture media to the culture wells. Culture media was changed every 3-4 days for 1 week. Cells seeded scaffolds were then either incubated in osteogenic media (OM) by adding 50 µg/mL of ascorbic acid and 10 mM β-glycerophosphate to the culture media or incubated in culture media (CM) for 2 weeks, with or without the application of hydrostatic pressure (HP).

Cyclic hydrostatic pressure stimulation

Cyclic hydrostatic pressure was applied by modulating the pressure in the gas phase above the culture wells in a custom-build pressure chamber (Figure 1, A). Briefly, the humidified, 95% air and 5% CO_2 incubator atmosphere was compressed using a commercial air compressor injected in the pressure chamber using solenoid valves. A Particle Photon microcontroller (Particle Industries, San Francisco, CA) was used to control the frequency and the duration of the applied pressure remotely via a custom-made cellphone application through Blynk IoT platform (Blynk, New York, NY)). Cyclic hydrostatic pressure stimulation was applied during 1 hour per day, for up to 2 weeks (Figure 1, B) at a frequency 1Hz, oscillating between 0 and 280 kPa with respect to ambient pressure. Pressure was monitored using a pressure transducer. The samples were removed from the pressure chamber after each cycle and kept at ambient pressure between the stimulation phases.

Cell-seeded scaffolds were either stimulated with cyclic hydrostatic pressure with and without the presence of osteogenic media, leading to four experimental conditions (Figure 1, B): Cyclic hydrostatic pressure in regular culture media (CHP), cyclic hydrostatic pressure in osteogenic culture media (CHP-OM), non-stimulated in osteogenic media (OM) and non-stimulated in regular culture media (control). The OM and control conditions were kept outside of the pressure chamber, in a humidified, 5% CO2 incubator at 37°C.

Scaffold imaging

After 1 week or 2 weeks, scaffolds were thoroughly washed with PBS and fixed with 10% neutral buffered formalin for 10 min. Scaffolds were washed with PBS and incubated in a 0.01% Congo Red staining solution (Sigma-Aldrich, St. Louis, MO) for 20 min at room temperature. Scaffolds were washed 3 times with PBS. Cell nuclei were stained with 1:1000 Hoechst (ThermoFisher, Waltham, MA) for 30 min in the dark. Samples were washed 3 times with PBS and stored in wash buffer solution (5% FBS in PBS) prior to imaging. The cell-seeded surface of the scaffolds was imaged with a high-speed resonant laser scanning confocal microscope (Nikon Ti-E A1-R) equipped with a 10X objective. Maximum intensity projections of the image slices were used for cell counting with ImageJ software (Schindelin et al., 2012). Cells were counted on a 1.3 by 1.3 mm^2 area (N=3 per experimental conditions with 3 randomly selected area per scaffold).

Alkaline phosphatase activity assay

Alkaline phosphatase (ALP) activity in media was measured using an ALP assay kit (BioAssay Systems, Hayward, CA). Briefly, a working solution was prepared to a 5 mM magnesium acetate and 10 mM p-nitrophenyl phosphate (pNPP) concentration in assay buffer, following manufacturer's protocol. 150 μL of working solution was pipetted in 96-well plate. 200 μL of calibrator solution and 200 μL of dH_2O were pipetted in separated well, in the same 96-well plate. At 1 week and 2 weeks, 20 μL of incubation media (either CM or OM) was pipetted into the working solution's well. All wells (samples, calibrator and dH_2O) were read at 405 nm for 10 minutes, every 30 seconds. ALP activity was calculated by taking the slope of the 405 nm readings vs time, calibrated with the calibrator solution and dH_2O. Wells were read in triplicates (N=3 per experimental conditions).

Alizarin red S staining and mineral deposit quantification

Samples were fixed with 10% neutral buffered formalin for 10 min, after 1 week or 2 weeks. Calcium quantification was performed using previously published protocol (Gregory et al., 2004). Briefly, samples were transferred to a 24-well plate and carefully washed with deionized water and incubated in 1 mL of 40mM (pH=4.1) alizarin red s (ARS, Sigma-Aldrich) solution for 20 minutes at room temperature, with light agitation. The samples were then washed 3x with deionized water and placed in 15 mL falcon tubes filled with 10 mL dH_2O. The tubes were placed on a rotary shaker at 120 rpm for 60 min and dH_2O was replaced every 15 min. Thereafter, samples were incubated in 800 µL of 10% acetic acid on an orbital shaker at 60 rpm for 30 min. The eluted ARS/acetic acid solution was pipettes out of the well and transferred to 1.5 mL centrifuge tubes. Tubes were centrifuged at 17 10^4 g for 15 min. 500 µL of supernatants were transferred to new centrifuge tube and 200 µL of 10% ammonium hydroxide was pipetted into the tubes. Finally, 150 µL of the solution was pipetted into a 96-well plate and the absorption at 405 was read using a plate reader (BioTek Instruments, Winooski, VT). Wells were read in triplicates (N=3 per experimental conditions).

Statistical analysis

Values reported in this manuscript are the average value ± standard error of the mean (SEM). Statistical significance was determined using one-way ANOVA and post hoc Tukey test. A value of $p < 0.05$ was considered to be statistically significant.

Results

Scaffold imaging and cell counting

Cell counting was performed on maximum projection of confocal slices (Figure 2). Data showed (Figure 2) significant increase in cellular density in scaffolds incubated in OM compared to CM, subjected to hydrostatic pressure after 1 week (723±80 cells/mm^2 and 353±71 cells/mm^2, respectively; p=0.02) but showed a non-significant increase after 2 weeks of stimulation (611±149 cells/mm^2 and 350±71 cells/mm^2, respectively; p=0.23). Non-significant increase was also observed in cellular density in scaffolds incubated in OM compared to CM, in the static case 1 week (125±27 cells/mm^2 and 88±16 cells/mm^2, respectively; p=0.99) and 2 weeks of stimulation (291±52 cells/mm^2 and 221±50 cells/mm^2, respectively; p=0.99). The application of hydrostatic pressure significantly increases the density of cells after for scaffolds incubated in OM after 1

week of stimulation compared to the static case (723±80 cells/mm^2 and 125±27 cells/mm^2, respectively; p=10^{-5}). An increase, non-significant, was also observed after 2 weeks of stimulation in similar conditions (611±149 cells/mm^2 and 291±52 cells/mm^2, respectively; p=0.07). Moreover, a non-significant increase in cellular density was observed by applied HP in scaffolds cultured in CM after 1 week (353±71 cells/mm^2 and 88±16 cells/mm^2, respectively; p=0.21) and 2 weeks of stimulation (350±71 cells/mm^2 and 221±50 cells/mm^2, respectively; p=0.92). In respective experimental condition, no significant change in the cell density were observed between the first and second week for scaffolds subjected to HP (723±80 cells/mm^2 and 611±149 cells/mm^2 for OM-HP scaffolds; p=0.96; 353±71 cells/mm^2 and 350±71 cells/mm^2 for CTRL-HP scaffolds; p=1). Finally, no significant change in the cell density were observed between the first and second week for scaffolds in the static case (125±27 cells/mm^2 and 291±52 cells/mm^2 for CM-HP scaffolds; p=1; 88±16 cells/mm^2 and 221±50 cells/mm^2 for CM-CTRL scaffolds; p=0.91).

Alkaline phosphatase activity assay

Alkaline phosphatase activity was assed by a pnpp kinetic reaction following manufacturer's protocol after 1 or 2 weeks (Figure 3). A significant increase in ALP activity was observed in scaffolds with applied hydrostatic pressure compared to the static case, incubated in osteogenic media after 1 week (0.245±0.003 IU/L and 0.189±0.002 IU/L, respectively; p=4x10^{-8}) and 2 weeks (0.214±0.002 IU/L and 0.159±0.002 IU/L, respectively; p=4x10^{-8}) of stimulation. Moreover the application of hydrostatic pressure also significantly increased the ALP activity in culture media after 1 week (0.203±0.001 IU/L and 0.195±0.001 IU/L, respectively; p=0.03) and 2 weeks (0.213±0.001 IU/L and 0.152±0.001 IU/L, respectively; p=5x10^{-8}). ALP activity significantly increased in samples incubated in osteogenic media compared to culture media with applied hydrostatic pressure after 1 week (0.245±0.003 IU/L and 0.203±0.001 IU/L, respectively; p<10^{-8}) but was not significantly different after 2 weeks (0.159±0.002 IU/L and 0.152±0.001 IU/L, respectively; p=0.99). Finally, ALP dis not significantly change in the absence of hydrostatic pressure for samples incubated in osteogenic media compared to culture media either at 1 week (0.189 ± 0.002 IU/L and 0.195 ± 0.001IU/L, respectively; p=0.25) or 2 weeks (0.159 ± 0.002 IU/L and 0.152 ± 0.001 IU/L, respectively; p=0.08).

Alizarin red S staining and mineral deposit quantification

ARS assay for quantifying mineralization was performed after 1 or 2 weeks (Figure 4). The application of hydrostatic pressure significantly increased the quantity of mineral deposition for both differentiation media (0.73±0.03 a.u. and 0.55±0.02 a.u., HP vs CTRL, respectively; p=2x10^{-7}) or culture media (0.59±0.03 a.u. and 0.42±0.02 a.u., HP vs CTRL, respectively; p=1x10^{-6}) at 1 week. The quantity of mineral deposition was also significantly increased after 2 weeks incubation in differentiation media (0.68±0.01 a.u. and 0.22±0.02 a.u., HP vs CTRL, respectively; p=2x10^{-8}) and culture media (0.69±0.02 a.u. and 0.17±0.02 a.u., HP vs CTRL, respectively; p=2x10^{-8}). The mineral deposition was also significantly increased by incubation in osteogenic media compared to culture media at 1 week for samples under hydrostatic pressure (0.73±0.03 a.u. and 0.59±0.03 a.u., OM vs CM; p=2x10^{-4}) and for non-compressed experiments (0.55±0.02 a.u. and 0.42±0.02 a.u., OM vs CM; p=10^{-3}). No significant change of mineral deposition was observed by incubation in osteogenic media compared to culture media at 2 weeks for samples under hydrostatic pressure (0.68±0.01 a.u. and 0.69±0.02 a.u., OM vs CM; p=0.99) and for non-compressed experiments (0.22±0.02 a.u. and 0.17±0.02 a.u., OM vs CM; p=0.75).

Discussion

Cells are known to react to different stimuli, such as tension, compression, shear forces ECM stiffness and ECM deformation (Vining and Mooney, 2017). These mechanotransduction stimuli are known to affect cell differentiation, tissue regeneration, cytokines and protein expression and proliferation (Martino et al., 2018; Vining and Mooney, 2017). Thus, adequate representation of physical environment is critical implant design in BTE (Campana et al., 2014; Gao et al., 2019; Nukavarapu et al., 2015; Parikh, 2002; Wang and Yeung, 2017). Bones are dynamical environment subjected to constant mechanical stresses. As consequence, bone adapt through remodeling process (Bonewald and Johnson, 2008). Osteoblasts responds to mechanical stimuli and remodel the bone architecture as a response (Lee and Volpicelli, 2017). *In vivo*, hydrostatic pressure is repeatedly stimulating bone cells and has shown to impact cell differentiation, makers expression and mineralisation of the bone tissue (Henstock et al., 2013; Huang and Ogawa, 2012; Reinwald and El Haj, 2018). As an emerging biomaterial in BTE (Lee et al., 2019), it is of importance to apply *in vivo* mechanical conditions to native cellulose scaffolds, as close matching of surrounding bone tissue as been shown to be the key factor in the success of alloplastic grafts (Gao et al., 2019; Nukavarapu et al., 2015). To our knowledge, cyclic hydrostatic effect of pre-osteoblast seeded on plant-derived scaffolds have not yet being studied. Cellulose biomaterials derived from plant tissues that closely match the physical environment has shown promising results *in vitro* and *in vivo* for targeted tissue engineering (Hickey et al., 2018; Modulevsky et al., 2016, 2014) and have been used to host mammalian osteoblastic differentiation in vivo and in vitro (Lee et al., 2019). In addition, apple-derived cellulose scaffolds exhibit similar morphological characteristics to trabecular bone and were previously used for BTE applications (Lee et al., 2019). Equivalent mechanical properties are preferable to avoid stress shielding effects at the bone-implant interface (Gao et al., 2019).

In this study, we further extend the investigation for this type of biomaterial by replicating the mechanical environment of human locomotion and measuring the impact of differentiation markers in seeded pre-osteoblast cells. External pressure was applied on the scaffolds in similar magnitude of the lacuna-canaliculi network with a frequency mimicking human locomotion (1Hz) (Henstock et al., 2013; Zhang et al., 1998). Scaffolds were seeded with pre-osteoblasts cells (MC3T3-E1). After proliferation, scaffolds were either cultured in standard culture media (CM), or in osteogenic-inducing differentiation media (OM). These scaffolds were then either subjected to cyclic hydrostatic pressure (HP) or kept at atmospheric pressure (CTRL) for 1 or 2 weeks. The applied HP was set at 1Hz for 1 hour per day, following a rest period at atmospheric pressure. Other groups using either similar cell line (Gardinier et al., 2014, 2009), human or animal bone marrow skeletal stem cells (BMSCs) (Reinwald and El Haj, 2018; Stavenschi et al., 2018; Zhao et al., 2015) or ex-vivo chick femur (Henstock et al., 2013) reports the effects of cyclic HP on either 2D surfaces, random or aligning PCL meshes or ex vivo bones. The aim of the study was to measure the effect of HP on Native Cellulose Scaffolds seeded with MC3T3-E1 cells. Cell counting by laser-scanning confocal microscopy revealed that the density of cells was significantly increased after 1 week and (non-significantly; $p=0.07$) 2 weeks of applied HP in osteogenic medium. An increase was also noted after 1 week and 2 weeks of applied HP in culture medium but was also non-significant. These results showed that the application of HP enhance MC3T3-E1 proliferation when cultured in OM. This result is corroborated by other studies (Reinwald and El Haj, 2018; Zhao et al., 2015). Human BMSCs metabolic activity was upregulates by mechanical stimulation (270 kPa; 1 Hz stimulation for 1h per day, for 5 days out of 2 weeks) in comparison to the non-stimulated samples (Reinwald and El Haj, 2018). Moreover, it was shown that the application of hydrostatic pressure on rat BMSCs accelerates cell proliferation through upregulated cell cycle initiation (Zhao et al., 2015). Similarly, reports showed that physical

stimulation of MC3T3-E1 cells induced expression of paracrine factors that leads enhancement of cell proliferation (Stavenschi et al., 2018). Physical stimulus thus affects the proliferation of cells in three-dimensional scaffolds.

The nature of incubation media influence on cellular density was illustrated by a significant increase in OM samples compared to CM samples after 1 week of HP, but a non-significant increase after 2 weeks in HP. Non-significant increase between OM and CM was observed for non-stimulated samples after 1 and weeks. Time-dependent, significant increase in MC3T3 cell number cultured in media containing ascorbic acid and β-glycerophosphate was also reported, followed by a time-dependent decrease in the replication rate (Quarles et al., 1992). No significant difference between incubation of MC3T3-E1 cells in similar osteogenic media after 2 weeks was also reported (Hong et al., 2010). Our findings corroborate these studies and further suggest that the application of HP influences the replication rate at early stages of stimulation for samples cultured in OM.

Alkaline phosphatase is an enzyme expressed in early staged of osteoblastic differentiation (Golub and Boesze-Battaglia, 2007). Our results indicate that the application of cyclic hydrostatic pressure significantly increases ALP activity of cell-seeded scaffolds, compared to the static case. These findings are consistent with other studies on more conventional scaffolds (Reinwald and El Haj, 2018). A significant increase in ALP activity was also noted by the incubation of the scaffolds in osteogenic-inducing differentiation media, similarly to reports on 2D culture systems (Hong et al., 2010; Quarles et al., 1992). The application of HP significantly increased the mineral content in the scaffolds after 1 week and 2 weeks of stimulation, in both types of incubation media. Other group have shown that a cyclic 300 kPa pressure at 2 Hz frequency on human BMSCs promoted significant mineral deposition (Stavenschi et al., 2018). The increase in mineral deposition also noted in ex vivo bone samples, with similar hydrostatic pressure force application (Henstock et al., 2013). Furthermore, the incubation in osteogenic media increased the mineral content in the scaffolds, which is consistent with other studies (Hong et al., 2010; Quarles et al., 1992). Along with ALP expression, mineral content expression further confirms the ongoing differentiation of MC3T3-E1 onto osteoblast, either by applied HP, chemically (induction in OM) or a combination of both.

Conclusion

Plant-derived scaffolds have demonstrated their efficiency for various biomedical and tissue engineering applications (Fontana et al., 2017; Gershlak et al., 2017; Hickey et al., 2018; Lee et al., 2019; Modulevsky et al., 2016, 2014). They are widely available, accessible and easily fabricated. The novelty, widespread availability, ease of use makes an interesting alternative to autografts, xenografts and synthetics implants. However, it has remined poorly understood how mechanosensitive pathways in bone precursor cells are impacted by being cultured in plant-derived cellulosic biomaterials. Previous studies have not included these phenomenon, either through mechanical loading or physical stimulation. In this study, mechanical stimulation of cell-seeded scaffolds and the subsequent cellular response allowed us to understand the implants mechanosensitive behaviors in these novel scaffolds. As bone tissues are highly dynamical environments, relevant forces should be considered in the implant design to treat injury or repair defects. Importantly, this work provides the early evidence that bone-precursor cells appear to possess intact mechanosensing and mechanotransduction pathways when cultured on plant-derived scaffolds in a mechanically active environment. The results obtained here are consistent with data on traditional scaffold choices. Cells were exposed to a cyclic pressure cycle (max

280kPa, 1Hz) for one hour per day, for a total of two weeks. The results reveal that application of hydrostatic pressure, in combination with osteogenic inducing media, leads to an increase in the number of cells, Alkaline phosphatase activity and mineralization over time. These results combined with past *in vitro* and *in vivo* studies using apple-derived scaffold biomaterials demonstrate their potential in BTE applications.

Acknowledgements

This work was supported by a Discovery Grant from the Natural Sciences and Engineering Research Council of Canada (NSERC) and a grant from the Li Ka Shing Foundation.

References

Andrzejowski, P., Giannoudis, P. V., 2019. The 'diamond concept' for long bone non-union management. J. Orthop. Traumatol. https://doi.org/10.1186/s10195-019-0528-0

Bonewald, L.F., Johnson, M.L., 2008. Osteocytes, mechanosensing and Wnt signaling. Bone. https://doi.org/10.1016/j.bone.2007.12.224

Brunelli, M., Perrault, C., Lacroix, D., 2019. A Review of Bioreactors and Mechanical Stimuli. Springer, Singapore, pp. 1–22. https://doi.org/10.1007/978-981-10-8075-3_1

Campana, V., Milano, G., Pagano, E., Barba, M., Cicione, C., Salonna, G., Lattanzi, W., Logroscino, G., 2014. Bone substitutes in orthopaedic surgery: from basic science to clinical practice. J. Mater. Sci. Mater. Med. 25, 2445–2461. https://doi.org/10.1007/s10856-014-5240-2

Di Martino, A., Sittinger, M., Risbud, M. V., 2005. Chitosan: A versatile biopolymer for orthopaedic tissue-engineering. Biomaterials. https://doi.org/10.1016/j.biomaterials.2005.03.016

Fernández, R.F., Bucchi, C., Navarro, P., Beltrán, V., Borie, E., 2015. Bone grafts utilized in dentistry: an analysis of patients' preferences. BMC Med. Ethics 16, 71. https://doi.org/10.1186/s12910-015-0044-6

Fontana, G., Gershlak, J., Adamski, M., Lee, J.-S., Matsumoto, S., Le, H.D., Binder, B., Wirth, J., Gaudette, G., Murphy, W.L., 2017. Biofunctionalized Plants as Diverse Biomaterials for Human Cell Culture. Adv. Healthc. Mater. 6, 1601225. https://doi.org/10.1002/adhm.201601225

Gao, X., Fraulob, M., Haïat, G., 2019. Biomechanical behaviours of the bone-implant interface: A review. J. R. Soc. Interface 16, 20190259. https://doi.org/10.1098/rsif.2019.0259

Gardinier, J.D., Gangadharan, V., Wang, L., Duncan, R.L., 2014. Hydraulic pressure during fluid flow regulates purinergic signaling and cytoskeleton organization of osteoblasts. Cell. Mol. Bioeng. 7, 266–277. https://doi.org/10.1007/s12195-014-0329-8

Gardinier, J.D., Majumdar, S., Duncan, R.L., Wang, L., 2009. Cyclic hydraulic pressure and fluid flow differentially modulate cytoskeleton re-organization in MC3T3 osteoblasts. Cell. Mol. Bioeng. 2, 133–143. https://doi.org/10.1007/s12195-008-0038-2

Gershlak, J.R., Hernandez, S., Fontana, G., Perreault, L.R., Hansen, K.J., Larson, S.A., Binder, B.Y.K., Dolivo, D.M., Yang, T., Dominko, T., Rolle, M.W., Weathers, P.J., Medina-Bolivar, F., Cramer, C.L., Murphy, W.L., Gaudette, G.R., 2017. Crossing kingdoms: Using decellularized plants as perfusable tissue engineering scaffolds. Biomaterials 125, 13–22. https://doi.org/10.1016/J.BIOMATERIALS.2017.02.011

Golub, E.E., Boesze-Battaglia, K., 2007. The role of alkaline phosphatase in mineralization. Curr. Opin. Orthop. 18, 444–448. https://doi.org/10.1097/BCO.0b013e3282630851

Gregory, C.A., Gunn, W.G., Peister, A., Prockop, D.J., 2004. An Alizarin red-based assay of mineralization by adherent cells in culture: Comparison with cetylpyridinium chloride extraction. Anal. Biochem. 329, 77–84. https://doi.org/10.1016/j.ab.2004.02.002
Henstock, J.R., Rotherham, M., Rose, J.B., El Haj, A.J., 2013. Cyclic hydrostatic pressure stimulates enhanced bone development in the foetal chick femur in vitro. Bone 53, 468–477. https://doi.org/10.1016/j.bone.2013.01.010
Hickey, R.J., Modulevsky, D.J., Cuerrier, C.M., Pelling, A.E., 2018. Customizing the Shape and Microenvironment Biochemistry of Biocompatible Macroscopic Plant-Derived Cellulose Scaffolds. ACS Biomater. Sci. Eng. 4, 3726–3736. https://doi.org/10.1021/acsbiomaterials.8b00178
Hickey, R.J., Pelling, A.E., 2019. Cellulose biomaterials for tissue engineering. Front. Bioeng. Biotechnol. https://doi.org/10.3389/fbioe.2019.00045
Hong, D., Chen, H.X., Yu, H.Q., Liang, Y., Wang, C., Lian, Q.Q., Deng, H.T., Ge, R.S., 2010. Morphological and proteomic analysis of early stage of osteoblast differentiation in osteoblastic progenitor cells. Exp. Cell Res. 316, 2291–2300. https://doi.org/10.1016/j.yexcr.2010.05.011
Huang, C., Ogawa, R., 2012. Effect of Hydrostatic Pressure on Bone Regeneration Using Human Mesenchymal Stem Cells. Tissue Eng. Part A 18, 2106–2113. https://doi.org/10.1089/ten.tea.2012.0064
Lee, J., Jung, H., Park, N., Park, S.H., Ju, J.H., 2019. Induced Osteogenesis in Plants Decellularized Scaffolds. Sci. Rep. 9, 1–10. https://doi.org/10.1038/s41598-019-56651-0
Lee, J.C., Volpicelli, E.J., 2017. Bioinspired Collagen Scaffolds in Cranial Bone Regeneration: From Bedside to Bench. Adv. Healthc. Mater. https://doi.org/10.1002/adhm.201700232
Liu, C., Zhao, Y., Cheung, W.Y., Gandhi, R., Wang, L., You, L., 2010. Effects of cyclic hydraulic pressure on osteocytes. Bone 46, 1449–1456. https://doi.org/10.1016/j.bone.2010.02.006
Martino, F., Perestrelo, A.R., Vinarský, V., Pagliari, S., Forte, G., 2018. Cellular mechanotransduction: From tension to function. Front. Physiol. https://doi.org/10.3389/fphys.2018.00824
Modulevsky, D.J., Cuerrier, C.M., Pelling, A.E., 2016. Biocompatibility of Subcutaneously Implanted Plant-Derived Cellulose Biomaterials. PLoS One 11, e0157894. https://doi.org/10.1371/journal.pone.0157894
Modulevsky, D.J., Lefebvre, C., Haase, K., Al-Rekabi, Z., Pelling, A.E., 2014. Apple derived cellulose scaffolds for 3D mammalian cell culture. PLoS One 9, e97835. https://doi.org/10.1371/journal.pone.0097835
Morrell, K.C., Hodge, W.A., Krebs, D.E., Mann, R.W., 2005. Corroboration of in vivo cartilage pressures with implications for synovial joint tribology and osteoarthritis causation. Proc. Natl. Acad. Sci. U. S. A. 102, 14819–14824. https://doi.org/10.1073/pnas.0507117102
Nukavarapu, S.P., Freeman, J.W., Laurencin, C.T., 2015. Regenerative Engineering of Musculoskeletal Tissues and Interfaces, Regenerative Engineering of Musculoskeletal Tissues and Interfaces. Elsevier Inc. https://doi.org/10.1016/C2014-0-02826-2
Parikh, S.N., 2002. Bone graft substitutes: past, present, future. J. Postgrad. Med. 48, 142–148.
Pörtner, R., Nagel-Heyer, S., Goepfert, C., Adamietz, P., Meenen, N.M., 2005. Bioreactor design for tissue engineering. J. Biosci. Bioeng. https://doi.org/10.1263/jbb.100.235
Quarles, L.D., Yohay, D.A., Lever, L.W., Caton, R., Wenstrup, R.J., 1992. Distinct proliferative and differentiated stages of murine MC3T3-E1 cells in culture: An in vitro model of osteoblast development. J. Bone Miner. Res. 7, 683–692. https://doi.org/10.1002/jbmr.5650070613
Reinwald, Y., El Haj, A.J., 2018. Hydrostatic pressure in combination with topographical cues affects the fate of bone marrow-derived human mesenchymal stem cells for bone tissue regeneration. J. Biomed. Mater. Res. - Part A 106, 629–640. https://doi.org/10.1002/jbm.a.36267

Reinwald, Y., Leonard, K.H.L., Henstock, J.R., Whiteley, J.P., Osborne, J.M., Waters, S.L., Levesque, P., El Haj, A.J., 2015. Evaluation of the growth environment of a hydrostatic force bioreactor for preconditioning of tissue-engineered constructs. Tissue Eng. - Part C Methods 21, 1–14. https://doi.org/10.1089/ten.tec.2013.0476

Sakkas, A., Wilde, F., Heufelder, M., Winter, K., Schramm, A., 2017. Autogenous bone grafts in oral implantology—is it still a “gold standard”? A consecutive review of 279 patients with 456 clinical procedures. Int. J. Implant Dent. 3. https://doi.org/10.1186/s40729-017-0084-4

Schindelin, J., Arganda-Carreras, I., Frise, E., Kaynig, V., Longair, M., Pietzsch, T., Preibisch, S., Rueden, C., Saalfeld, S., Schmid, B., Tinevez, J.-Y., White, D.J., Hartenstein, V., Eliceiri, K., Tomancak, P., Cardona, A., 2012. Fiji: an open-source platform for biological-image analysis. Nat. Methods 9, 676–682. https://doi.org/10.1038/nmeth.2019

Stavenschi, E., Corrigan, M.A., Johnson, G.P., Riffault, M., Hoey, D.A., 2018. Physiological cyclic hydrostatic pressure induces osteogenic lineage commitment of human bone marrow stem cells: A systematic study. Stem Cell Res. Ther. 9. https://doi.org/10.1186/s13287-018-1025-8

Torgbo, S., Sukyai, P., 2018. Bacterial cellulose-based scaffold materials for bone tissue engineering. Appl. Mater. Today 11, 34–49. https://doi.org/10.1016/J.APMT.2018.01.004

Vining, K.H., Mooney, D.J., 2017. Mechanical forces direct stem cell behaviour in development and regeneration. Nat. Rev. Mol. Cell Biol. https://doi.org/10.1038/nrm.2017.108

Wang, W., Yeung, K.W.K., 2017. Bone grafts and biomaterials substitutes for bone defect repair: A review. Bioact. Mater. https://doi.org/10.1016/j.bioactmat.2017.05.007

Wei, S., Ma, J.X., Xu, L., Gu, X.S., Ma, X.L., 2020. Biodegradable materials for bone defect repair. Mil. Med. Res. https://doi.org/10.1186/s40779-020-00280-6

Zhang, D., Weinbaum, S., Cowin, S.C., 1998. Estimates of the peak pressures in bone pore water. J. Biomech. Eng. 120, 697–703. https://doi.org/10.1115/1.2834881

Zhao, Y.H., Lv, X., Liu, Y.L., Zhao, Y., Li, Q., Chen, Y.J., Zhang, M., 2015. Hydrostatic pressure promotes the proliferation and osteogenic/chondrogenic differentiation of mesenchymal stem cells: The roles of RhoA and Rac1. Stem Cell Res. 14, 283–296. https://doi.org/10.1016/j.scr.2015.02.006

FIGURE LEGENDS

Figure 1: (A) Cyclic hydrostatic pressure device schematics. Hydrostatic pressure was applied by modulating the pressure in the gas phase above the culture wells in a custom-build pressure chamber. Air from incubator atmosphere was compressed using a compressor and injected in the pressure chamber using solenoid valves. (B) Experimental conditions. After 1 week of proliferation, cyclic hydrostatic pressure stimulation was applied during 1 hour per day, for up to 2 weeks at a frequency 1Hz, oscillating between 0 and 280 kPa with respect to ambient pressure. The samples were removed from the pressure chamber after each cycle and kept at ambient pressure between the stimulation phases.

Figure 2: (A) Representative confocal laser scanning microscope image showing seeded cells scaffolds (scale bar = 100 µm – applies to all). The scaffolds were stained for cellulose (red) and for cell nuclei (blue). (B) Cellular density after 1 week or 2 weeks of stimulation. Statistical significance (* indicates $p<0.05$) was determined using a one-way ANOVA and Tukey post-hoc tests. Data are presented as means ± S.E.M. of three replicate samples per condition, with three areas per sample.

Figure 3: Alkaline phosphatase (ALP) activity after 1 week or 2 weeks of stimulation. Statistical significance (* indicates $p<0.05$) was determined using a one-way ANOVA and Tukey post-hoc tests. Data are presented as means ± S.E.M. of three replicate samples per condition.

Figure 4: Mineral deposit quantification with Alizarin Red S (ARS) staining after 1 week or 2 weeks of stimulation. Statistical significance (* indicates $p<0.05$) was determined using a one-way ANOVA and Tukey post-hoc tests. Data are presented as means ± S.E.M. of three replicate samples per condition.

FIGURE 1

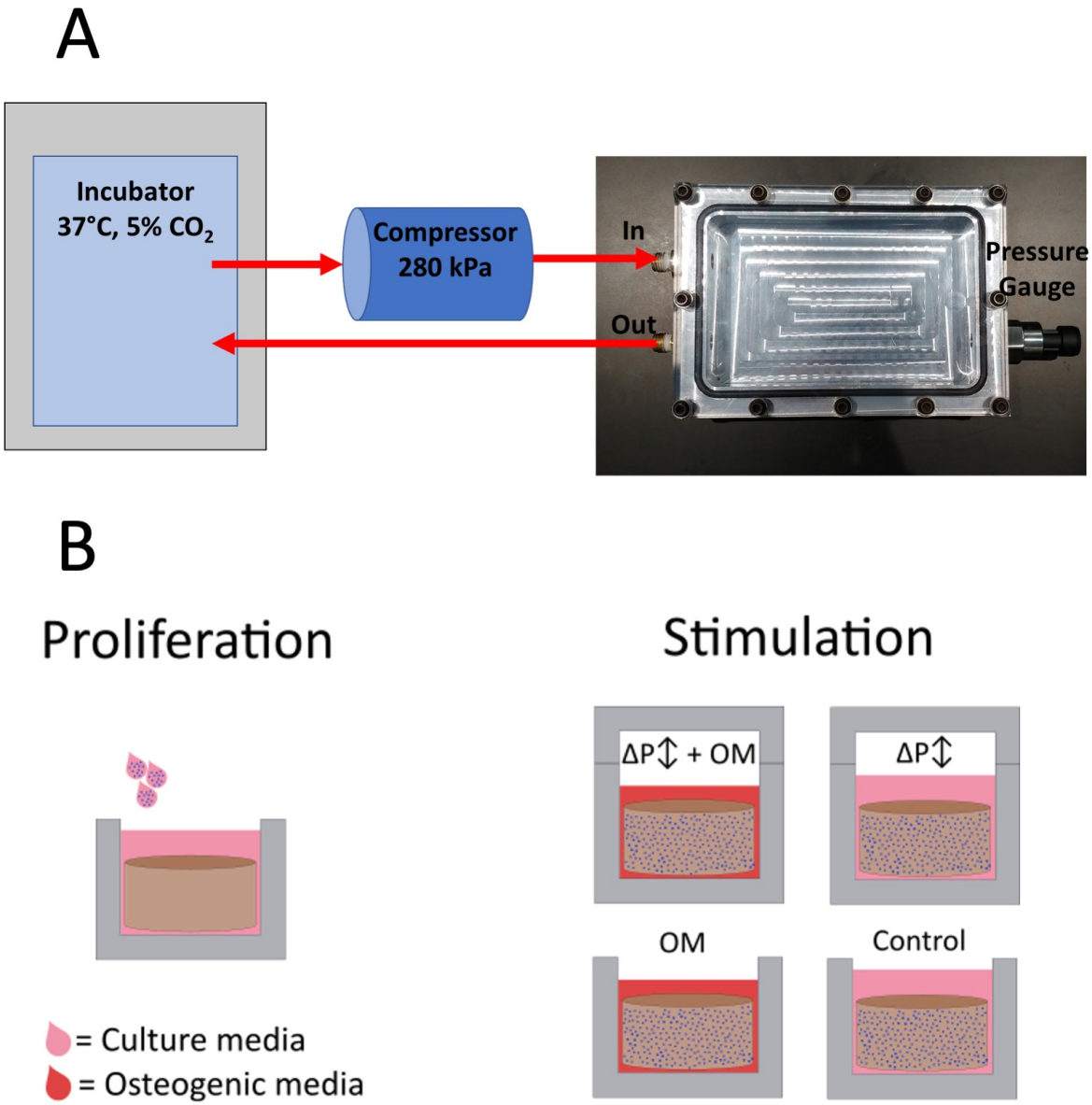
A
Incubator
37°C, 5% CO_2
Compressor
280 kPa
In
Out
Pressure
Gauge
B
Proliferation
Stimulation
ΔP↕ + OM
ΔP↕
OM
Control
= Culture media
= Osteogenic media

FIGURE 2

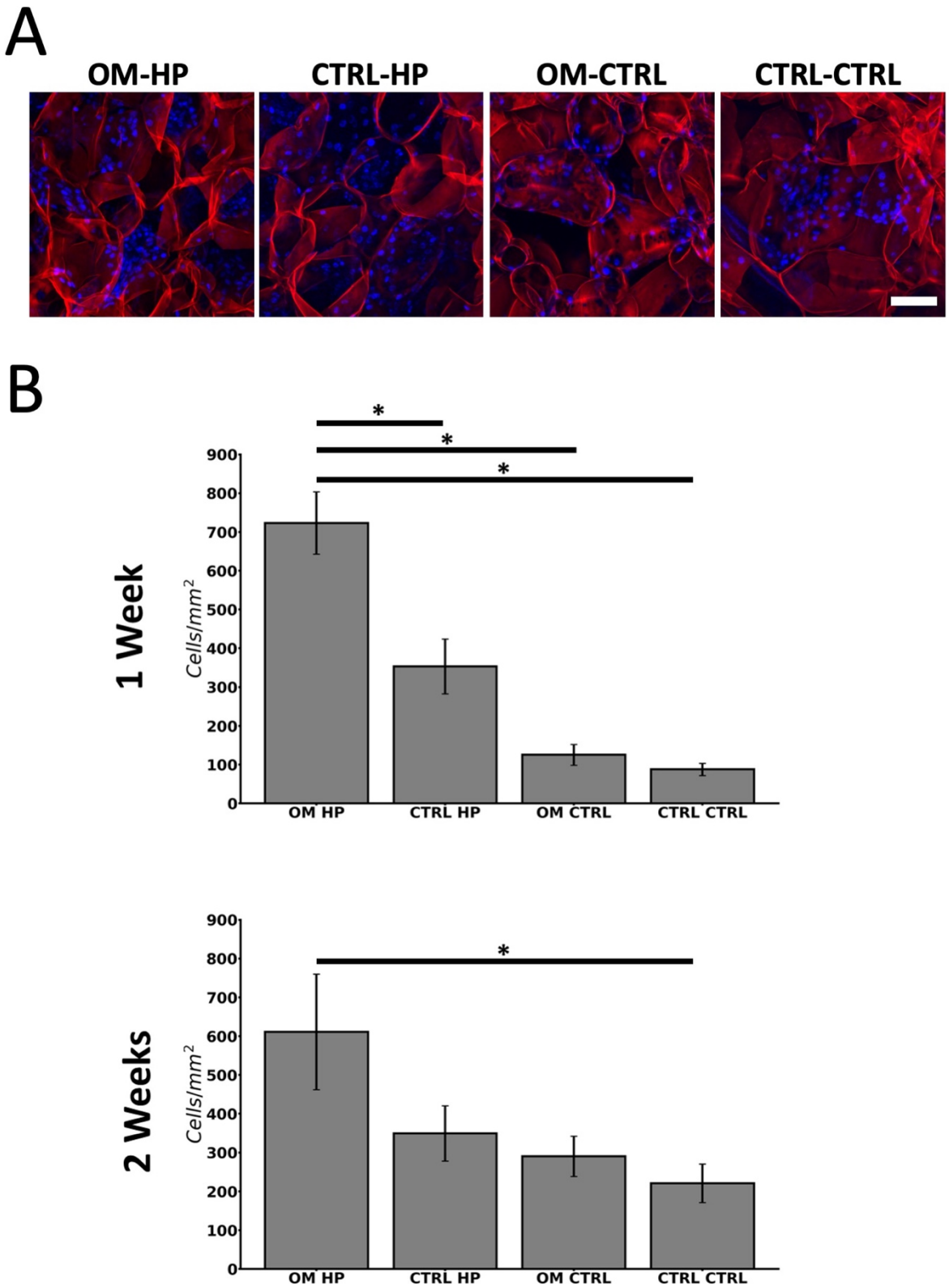
A
OM-HP
CTRL-HP
OM-CTRL
CTRL-CTRL
B
1 Week
Cells/mm²
900
800
700
600
500
400
300
200
100
0
OM HP
CTRL HP
OM CTRL
CTRL CTRL
*
*
*
2 Weeks
Cells/mm²
900
800
700
600
500
400
300
200
100
0
OM HP
CTRL HP
OM CTRL
CTRL CTRL
*

FIGURE 3

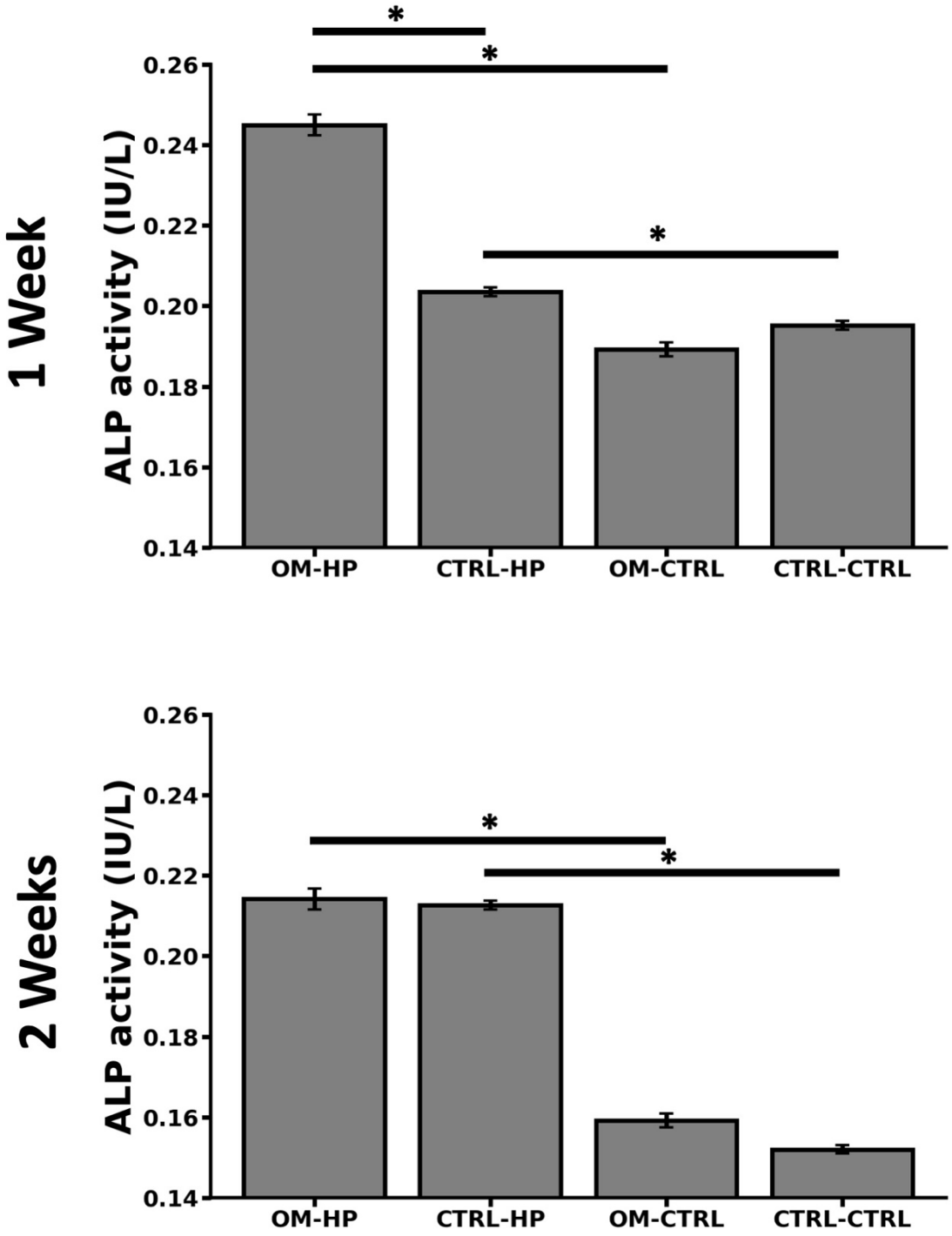
1 Week
ALP activity (IU/L)
0.26
0.24
0.22
0.20
0.18
0.16
0.14
*
*
*
OM-HP
CTRL-HP
OM-CTRL
CTRL-CTRL
2 Weeks
ALP activity (IU/L)
0.26
0.24
0.22
0.20
0.18
0.16
0.14
*
*
OM-HP
CTRL-HP
OM-CTRL
CTRL-CTRL

FIGURE 4

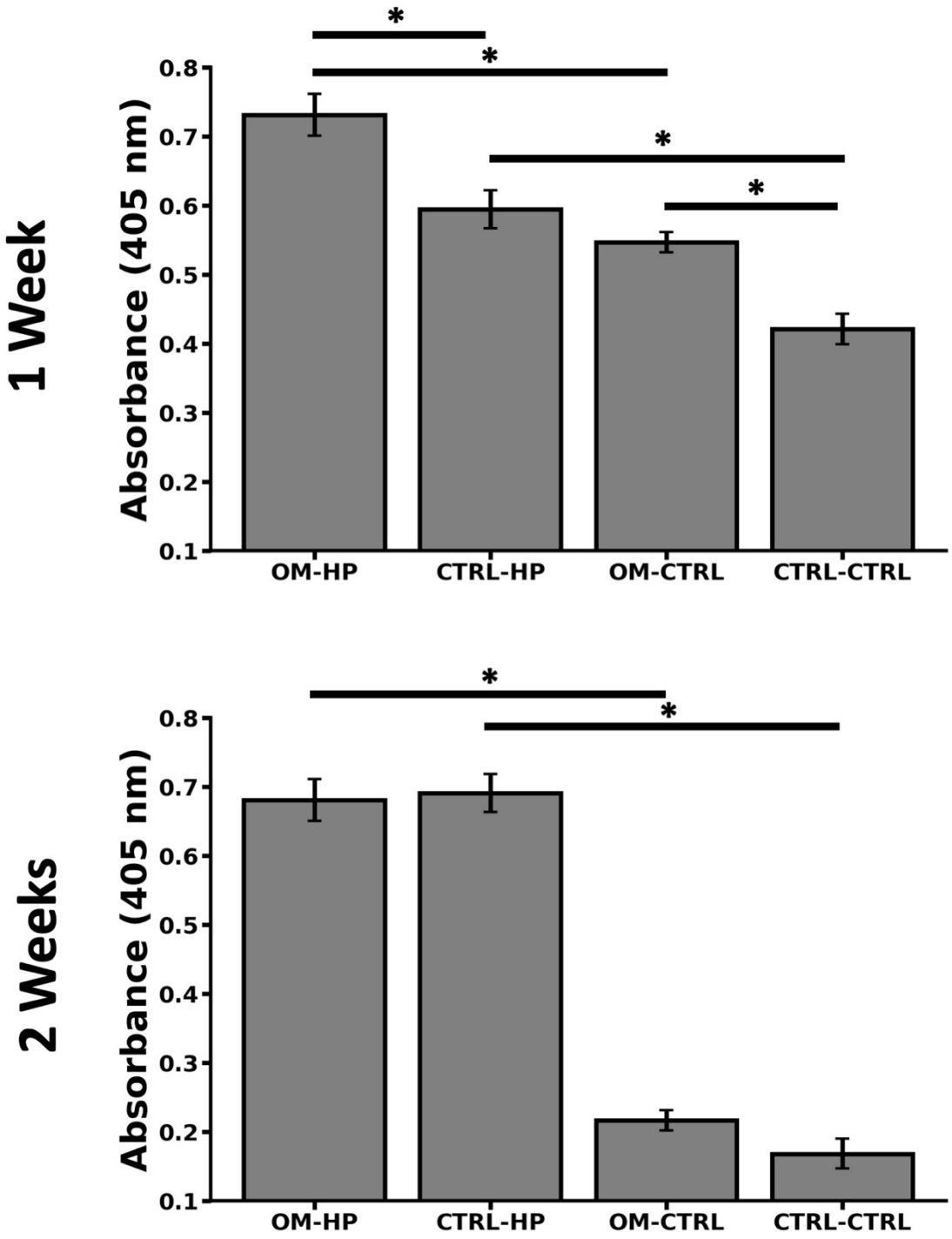
1 Week
Absorbance (405 nm)
0.8
0.7
0.6
0.5
0.4
0.3
0.2
0.1
*
*
*
*
OM-HP
CTRL-HP
OM-CTRL
CTRL-CTRL
2 Weeks
Absorbance (405 nm)
0.8
0.7
0.6
0.5
0.4
0.3
0.2
0.1
*
*
OM-HP
CTRL-HP
OM-CTRL
CTRL-CTRL